Generalized EXIT Chart and BER Analysis of Finite-Length Turbo Codes

Jeong W. Lee and Richard E. Blahut
University of Illinois at Urbana-Champaign
1308 W. Main St., Urbana, IL 61801, USA
Email: jwlee2, blahut@uiuc.edu

***Abstract*— We propose an analysis tool of the finite-length iterative turbo decoding algorithm. The proposed tool is a generalized EXIT chart based on the mutual information transfer characteristics of the extrinsic information in the iterative turbo decoding algorithm. The proposed tool can describe the probabilistic convergence behavior of the iterative decoding algorithm. By using this tool, we obtain the BER estimates of the finite-length turbo codes in the form of a lower bound, which shows a gentle waterfall over a wide waterfall region. The obtained lower bound is in reasonable agreement with the BER obtained by the simulations of the iterative decoding algorithm.**

I. Introduction

Since turbo codes were introduced [1] by Berrou *et al.* in 1993, the analysis of the bit error rate (BER) performance has been an important issue. However, due to the mathematical complexity of the iterative turbo decoding algorithm, the analytical derivation of the BER performance has not been successful and thus we usually rely on extensive simulations. As an alternative to avoid the exhaustive simulation, ten Brink [2] proposed the extrinsic information transfer (EXIT) chart considering the mutual information transfer characteristics of the extrinsic information in each constituent soft-in/soft-out (SISO) decoder of the turbo decoding algorithm under the Gaussian assumption of the input extrinsic information with a consistent probability density function (pdf) [3]. Independently, El Gamal and Hammons [4], and Divsalar *et al* [5] proposed a similar analysis tool using the signal-to-noise ratio (SNR) transfer characteristics of the Gaussian extrinsic information. These tools are useful to predict the threshold $\frac{E_b}{N_0}$, where the waterfall occurs in the BER performance, of the infinite-length turbo codes. However, the information blocklength of turbo codes is, in practice, limited to avoid the high communication latency and the high decoding complexity, e.g., 40 to 5114 bits per information block is chosen in the 3G communications [6]. Since the finite-length turbo codes have a BER performance with a gentle waterfall over a wide waterfall region, the threshold $\frac{E_b}{N_0}$ is not that meaningful and thus the EXIT chart and the SNR transfer chart are not that useful for the analysis of the finite-length turbo decoding algorithm. Thus, there has been the need for an analysis tool of the finite-length turbo codes and decoding algorithm. Lee and Blahut [7], [8] proposed

This work was supported by NSF CCR 99-79381 and NSF ITR 00-85929.

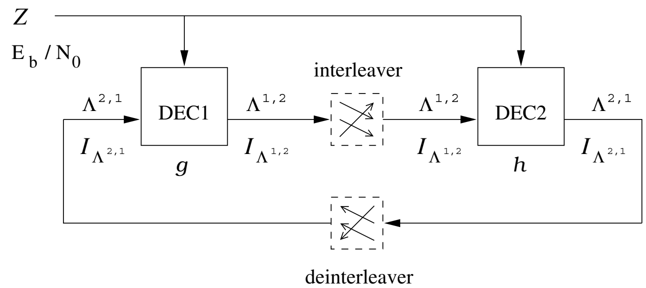

Fig. 1. The structure of turbo decoding algorithm, where Z represents the channel output or the received codeword frame, $\Lambda^{1,2}$ and $\Lambda^{2,1}$ denote the extrinsic information obtained in DEC1 and DEC2, respectively.

the SNR transfer characteristic band (TCB) chart to analyze the finite-length turbo decoding algorithm and obtain the BER estimate or the lower bound on the BER performance of the finite-length turbo codes. In an analogous manner, in this paper, we propose an EXIT band chart which can give the information about the probabilistic convergence behavior of the iterative decoding algorithm. Then, we obtain a lower bound on the average BER performance of the finite-length turbo codes by using the EXIT band chart. The obtained lower bound is in reasonable agreement with the BER performance obtained by the full simulation of the iterative decoding algorithm even in the wide waterfall region.

II. Turbo Decoding Preliminaries

The iterative turbo decoding uses the maximum *a posteriori* probability (MAP) decision algorithm composed of two constituent SISO decoders [1], which are named as DEC1 and DEC2, respectively. The extrinsic information messages obtained in one constituent SISO decoder are fed back to the next constituent SISO decoder after interleaved or deinterleaved to be used as the prior messages as shown in Fig. 1. Thus, the behavior of each constituent SISO decoder can be represented as a function of the extrinsic information for given received codeword frame, or the channel output sequence. Throughout this paper, we assume a binary additive white Gaussian noise (AWGN) channel and the binary phase shift keying (BPSK) signalling which maps the information bit 0 and 1 to 1 and -1, respectively. Then, without loss of generality, we assume the all-zero information sequence which is transmitted as the all-one sequence. Let b_k, $k = 1, 2, \cdots, N$, denote the information bit in the information block with length N, and let x_k be the channel output of the BPSK signal corresponding to b_k. Then, we can write down the posterior ℓ_k of b_k in the turbo decoding algorithm in an AWGN channel with the noise variance σ^2 as [1]

$$\ell_k = \frac{2}{\sigma^2} x_k + \lambda_k^{1,2} + \lambda_k^{2,1}, \quad k = 1, 2, \cdots, N, \tag{1}$$

where $\lambda_k^{1,2}$ and $\lambda_k^{2,1}$ denote the extrinsic information of b_k obtained in DEC1 and DEC2, respectively.

III. EXIT Band Chart

It is known that the behavior of each constituent SISO decoder in the infinite-length turbo decoding algorithm can be represented [2] by the transfer characteristics of the extrinsic information in terms of the mutual information between the extrinsic information and the corresponding information bit. In this Section, we propose a more general transfer characteristics of the extrinsic information to be used for the analysis of the finite-length iterative turbo decoding algorithm. It is observed that the sequence of extrinsic information has an approximately Gaussian histogram [8]. Thus, the sequence of extrinsic information for each received codeword frame associated with a certain channel realization and interleaver will be regarded as an observation sequence of a Gaussian random variable with a consistent pdf [3]. Let $[s]$ label the seed of channel realization and interleaver. Then, for given $[s]$, we obtain the sequences of output extrinsic information, $\{\lambda_k^{1,2^{[s]}}\}_{k=1}^N$ in DEC1 and $\{\lambda_k^{2,1^{[s]}}\}_{k=1}^N$ in DEC2. By the consistent pdf of extrinsic information, the variance is twice the mean so the statistics of extrinsic information can be described only by the SNR, where SNR is half the mean and one quarter of the variance. Let $\mathrm{snr}_{\Lambda^{1,2[s]}}$ and $\mathrm{snr}_{\Lambda^{2,1[s]}}$ be the SNR of the sequence $\{\lambda_k^{1,2^{[s]}}\}_{k=1}^N$ and $\{\lambda_k^{2,1^{[s]}}\}_{k=1}^N$, respectively. As mentioned above, for given $[s]$, we can interpret $\{\lambda_k^{1,2^{[s]}}\}_{k=1}^N$ and $\{\lambda_k^{2,1^{[s]}}\}_{k=1}^N$ as the observation sequence of the Gaussian random variable $\Lambda^{1,2^{[s]}} \sim \mathcal{N}\left(2\mathrm{snr}_{\Lambda^{1,2[s]}}, 4\mathrm{snr}_{\Lambda^{1,2[s]}}\right)$ and $\Lambda^{2,1^{[s]}} \sim \mathcal{N}\left(2\mathrm{snr}_{\Lambda^{2,1[s]}}, 4\mathrm{snr}_{\Lambda^{2,1[s]}}\right)$, respectively. In the iterative decoding process, $\Lambda^{1,2^{[s]}}$ and $\Lambda^{2,1^{[s]}}$ are also used as the input extrinsic information of DEC2 and DEC1, respectively. Let $I_{\Lambda^{1,2[s]}}$ be the mutual information between the extrinsic information $\Lambda^{1,2^{[s]}}$ and the information bit. When $\Lambda^{1,2^{[s]}}$ is considered the input extrinsic information of DEC2, $I_{\Lambda^{1,2[s]}}$ is related with $\mathrm{snr}_{\Lambda^{1,2[s]}}$ as [2]

$$I_{\Lambda^{1,2[s]}} = J\left(\mathrm{snr}_{\Lambda^{1,2[s]}}\right), \tag{2}$$

where

$$J(x) = 1 - \int_{-\infty}^{\infty} \frac{1}{\sqrt{8\pi x}} \exp\left(-\frac{(y-2x)^2}{8x}\right) \cdot \log_2\left(1 + e^{-y}\right) dy \tag{3}$$

with $x \geq 0$ is an increasing function. On the other hand, when $\Lambda^{1,2^{[s]}}$ is considered the output extrinsic information of DEC1,

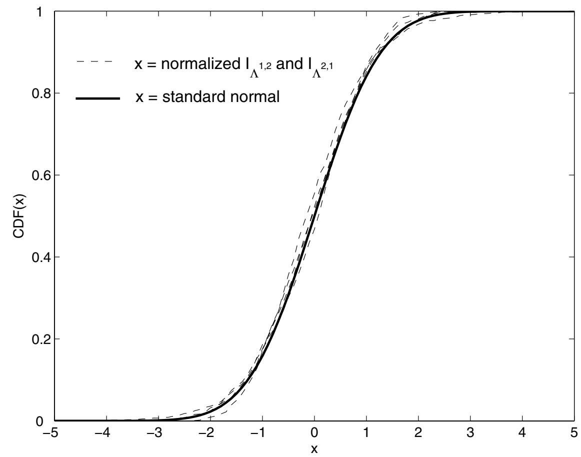

Fig. 2. The cumulative distribution of the normalized $I_{\Lambda^{1,2}}$ [or $I_{\Lambda^{2,1}}$] for arbitrarily fixed $I_{\Lambda^{2,1}}$ [or $I_{\Lambda^{1,2}}$] and $\frac{E_b}{N_0}$ in DEC1 [or DEC2] with $G = (23, 35)$, $N = 1024$ and $R_c = 1/2$.

$I_{\Lambda^{1,2[s]}}$ is obtained by using the histogram of $\{\lambda_k^{1,2^{[s]}}\}_{k=1}^N$. The mutual information between the information bit and the extrinsic information $\Lambda^{2,1^{[s]}}$, which is denoted by $I_{\Lambda^{2,1[s]}}$, is obtained in the same manner as for $I_{\Lambda^{1,2[s]}}$. Consequently, for a given seed of channel realization and interleaver labelled with $[s]$, the behavior of each constituent SISO decoder can be described by the transfer characteristics of the mutual information $I_{\Lambda^{1,2}}$ and $I_{\Lambda^{2,1}}$ with a parameter $\frac{E_b}{N_0}$ as

$$I_{\Lambda^{1,2[s]}} = g^{[s]}\left(I_{\Lambda^{2,1}}, \frac{E_b}{N_0}\right) \qquad \text{for DEC1} \tag{4}$$

$$I_{\Lambda^{2,1[s]}} = h^{[s]}\left(I_{\Lambda^{1,2}}, \frac{E_b}{N_0}\right) \qquad \text{for DEC2.} \tag{5}$$

Since the functions $g^{[s]}$ and $h^{[s]}$ cannot be analytically derived in practice, we obtain those functions by using the open loop simulation [7] without considering iterations. We repeat the open loop simulation by changing the seed of the channel realization and the sequence of input extrinsic information in order to simulate the various channel realization and interleavers used in the actual iterative turbo decoding process. Since the change of the seed for the sequence of input extrinsic information can simulate the change of the interleaver used in the actual iterative turbo decoding process, we can also label the seed of the channel realization and the sequence of input extrinsic information by $[s]$. We obtain various values for the mutual information of output extrinsic information in the constituent SISO decoder depending on the seed of the channel realization and the sequence of input extrinsic information even though we use the same $\frac{E_b}{N_0}$ and the same mutual information of input extrinsic information. Thus, for each $\frac{E_b}{N_0}$, by plotting the collection of $I_{\Lambda^{1,2}}$ [or $I_{\Lambda^{2,1}}$] with respect to $I_{\Lambda^{2,1}}$ [or $I_{\Lambda^{1,2}}$] in DEC1 [or DEC2], a band of $I_{\Lambda^{1,2}}$ [or $I_{\Lambda^{2,1}}$] called the EXIT band is obtained. It is observed that in DEC1 [or DEC2], $I_{\Lambda^{1,2}}$ [or $I_{\Lambda^{2,1}}$] has approximately a Gaussian histogram for each $\frac{E_b}{N_0}$ and each $I_{\Lambda^{2,1}}$ [or $I_{\Lambda^{1,2}}$] as shown in Fig. 2. Thus, for

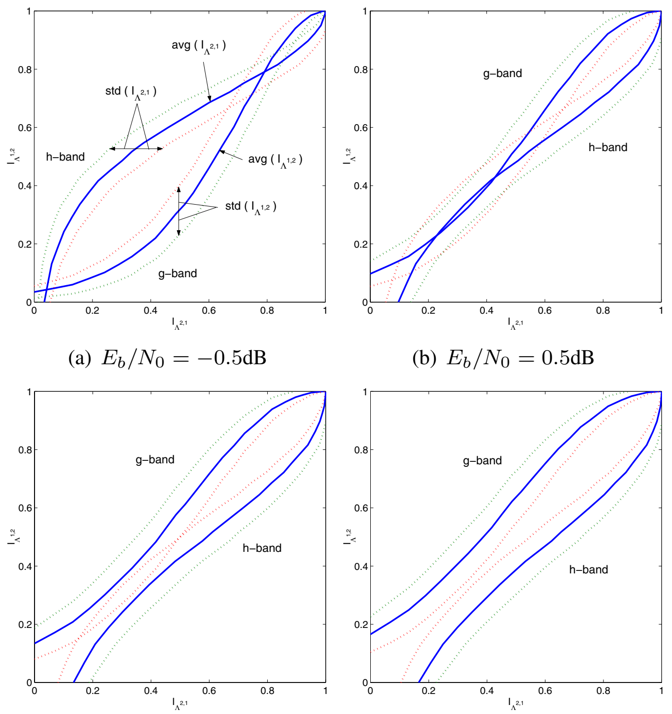

(a) $E_b/N_0 = -0.5$dB (b) $E_b/N_0 = 0.5$dB

(c) $E_b/N_0 = 0.8$dB (d) $E_b/N_0 = 1$dB

Fig. 3. The EXIT band chart of the turbo decoding algorithm with $G = (31, 27)$, $N = 1024$ and $R = 1/2$.

each $\frac{E_b}{N_0}$, the band of $I_{\Lambda^{1,2}}$ [or $I_{\Lambda^{2,1}}$] for DEC1 [or DEC2] can be represented by $\mathrm{avg}(I_{\Lambda^{1,2}})$ and $\mathrm{avg}(I_{\Lambda^{1,2}}) \pm \mathrm{std}(I_{\Lambda^{1,2}})$ [or $\mathrm{avg}(I_{\Lambda^{2,1}})$ and $\mathrm{avg}(I_{\Lambda^{2,1}}) \pm \mathrm{std}(I_{\Lambda^{2,1}})$] as shown in Fig. 3, where $\mathrm{avg}(\cdot)$ and $\mathrm{std}(\cdot)$ denote the average and the standard deviation, respectively. The obtained two EXIT bands corresponding to DEC1 and DEC2 are plotted together in one plane as shown in Fig. 3, which is named as the EXIT band chart. For each $\frac{E_b}{N_0}$ and $I_{\Lambda^{2,1}}$ [or $I_{\Lambda^{1,2}}$], we can choose one $I_{\Lambda^{1,2}}$ [or $I_{\Lambda^{2,1}}$] out of all possible ones in the EXIT band corresponding to DEC1 [or DEC2]. By interpolating chosen $I_{\Lambda^{1,2}}$ [or $I_{\Lambda^{2,1}}$], we can obtain a mutual information transfer characteristic of the input and output extrinsic information in DEC1 [or DEC2] for an arbitrarily chosen seed of channel realization and interleaver. Then, the EXIT band for DEC1 and DEC2 can be thought to contain many mutual information transfer characteristics $g^{[s]}$ and $h^{[s]}$, respectively, obtained for various seeds of channel realization and interleaver. Thus, we can also call these two EXIT bands as the g-band and the h-band, respectively. Fig. 4 shows the mutual information trajectories of the individual sequences of extrinsic information obtained from the iterative turbo decoding simulation. This shows that the individual mutual information trajectories fit in the EXIT band chart quite well, where we note that the EXIT bands are represented by the statistical bands as mentioned above. The widths of g-band and h-band depend on the information blocklength N reciprocally. As N goes to infinity, the widths of g-band and h-band go to zero so the EXIT band chart shrinks to the ordinary EXIT chart.

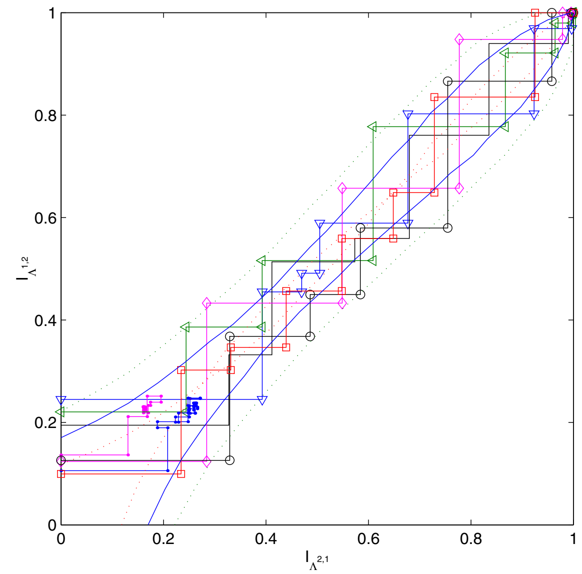

Fig. 4. The mutual information trajectories and the EXIT band chart, where $N = 1024$, $G = (15, 13)$, $R_c = 1/2$ and $E_b/N_0 = 0.8$dB.

The g-band and the h-band are monotonically increasing with respect to $I_{\Lambda^{2,1}}$ and $I_{\Lambda^{1,2}}$, respectively. Since the first intersection of $g^{[s]}$ and $h^{[s]}$ implies the convergence of the iterative decoding algorithm for given seed of channel realization and interleaver labelled with $[s]$, the study of the intersection behavior of g-band and h-band can give us the information on the probabilistic convergence behavior of the iterative decoding algorithm. For very low $\frac{E_b}{N_0}$ as shown in Fig. 3 (a), the g-band and the h-band intersect at low $I_{\Lambda^{1,2}}$ and $I_{\Lambda^{2,1}}$ with high probability, which results in high BER. As $\frac{E_b}{N_0}$ grows, the probability that the g-band and the h-band intersect at low $I_{\Lambda^{1,2}}$ and $I_{\Lambda^{2,1}}$ decreases slowly, which causes a slow improvement in the BER performance with respect to $\frac{E_b}{N_0}$ and thus a wide waterfall region. At very high $\frac{E_b}{N_0}$, the g-band and the h-band intersect at high $I_{\Lambda^{1,2}}$ and $I_{\Lambda^{2,1}}$ with probability 1, which results in the low BER performance.

IV. Lower Bound on BER Performance

In Section III, we showed that the proposed EXIT band chart is useful for the qualitative analysis of the finite-length iterative turbo decoding algorithm. In this Section, we will show that the proposed EXIT band chart is useful for the quantitative analysis as well. For given $[s]$, we obtain the AWGN channel output $x_k^{[s]}$ which is regarded as the kth observation of a Gaussian random variable $X^{[s]} \sim \mathcal{N}(1, \sigma^2)$. Then, for given $[s]$, (1) can be written as

$$\ell_k^{[s]} = \frac{2}{\sigma^2} x_k^{[s]} + \lambda_k^{1,2^{[s]}} + \lambda_k^{2,1^{[s]}}. \quad (6)$$

Since for given $[s]$, the channel output sequence and the sequences of extrinsic information are regarded as the observation sequences of Gaussian random variables as mentioned above, the sequence of posterior $\{\ell_k^{[s]}\}_{k=1}^N$ can also be regarded as the observation sequence of a Gaussian random variable. In other words, we can regard $\ell_k^{[s]}$, $x_k^{[s]}$, $\lambda_k^{1,2[s]}$ and $\lambda_k^{2,1[s]}$ as the kth observations of the Gaussian random variables $L^{[s]}$, $X^{[s]}$, $\Lambda^{1,2[s]}$ and $\Lambda^{2,1[s]}$, respectively. It is accepted that $X^{[s]}$, $\Lambda^{1,2[s]}$ and $\Lambda^{2,1[s]}$ are weakly and nonnegatively correlated. Under the assumption that the all-one sequence is transmitted, the mean of $L^{[s]}$ is written as

$$\mu_{L^{[s]}} = 4R_c\frac{E_b}{N_0} + 2\mathrm{snr}_{\Lambda^{1,2[s]}} + 2\mathrm{snr}_{\Lambda^{2,1[s]}}, \tag{7}$$

where $\frac{1}{\sigma^2} = 2R_c\frac{E_b}{N_0}$. By the nonnegative correlation of $X^{[s]}$, $\Lambda^{1,2[s]}$ and $\Lambda^{2,1[s]}$, the variance of $L^{[s]}$ is lower-bounded as

$$\sigma^2_{L^{[s]}} \geq 8R_c\frac{E_b}{N_0} + 4\mathrm{snr}_{\Lambda^{1,2[s]}} + 4\mathrm{snr}_{\Lambda^{2,1[s]}} = 2\mu_{L^{[s]}}. \tag{8}$$

From now on, we consider a fixed $\frac{E_b}{N_0}$ for a simple notation, where all variables, in fact, depend on $\frac{E_b}{N_0}$. Let $P_e^{[s]}$ be the bit error probability for given $[s]$, where $P_e^{[s]}$ is regarded as the sth observation of the random variable P_e. Since the turbo decoding algorithm uses the sign of the posterior, $P_e^{[s]}$ can be computed by

$$P_e^{[s]} = Q\left(\frac{\mu_{L^{[s]}}}{\sigma_{L^{[s]}}}\right), \tag{9}$$

where $Q(x) = \int_x^\infty \frac{1}{\sqrt{2\pi}}e^{-\frac{t^2}{2}}dt$. Since $\frac{\mu_{L^{[s]}}}{\sigma_{L^{[s]}}} \leq \sqrt{2R_c\frac{E_b}{N_0} + \mathrm{snr}_{\Lambda^{1,2[s]}} + \mathrm{snr}_{\Lambda^{2,1[s]}}}$ by (7) and (8), and $Q(\cdot)$ is a decreasing function, it follows from (2) and (9) that the BER performance for given $[s]$ is lower bounded as

$$P_e^{[s]} \geq Q\left(\sqrt{2R_c\frac{E_b}{N_0} + J^{-1}\left(I_{\Lambda^{1,2[s]}}\right) + J^{-1}\left(I_{\Lambda^{2,1[s]}}\right)}\right). \tag{10}$$

Now, let us consider the lower bound on the average BER performance over all possible channel realization and interleavers by using the EXIT band chart. Since the constant sum of $J^{-1}\left(I_{\Lambda^{1,2}}\right)$ and $J^{-1}\left(I_{\Lambda^{2,1}}\right)$ makes the right hand side (RHS) of (10) constant, we regard the curve $J^{-1}\left(I_{\Lambda^{1,2}}\right) + J^{-1}\left(I_{\Lambda^{2,1}}\right) = K$ with a constant K as the "equi-BER contour". For given K, let us define t_K coordinates whose axis is the equi-BER contour. This relationship is depicted in Fig. 5. For given K, let $v_K : t \mapsto I_{\Lambda^{1,2}}$, where $v_K(\cdot)$ is monotonically decreasing and t is the value of a point on the t_K axis. For given K, let us define a random variable A_K which denotes the point on the segment of $J^{-1}\left(I_{\Lambda^{1,2}}\right) + J^{-1}\left(I_{\Lambda^{2,1}}\right) = K$ intersecting the g-band, where the observation values of A_K are read in the t_K coordinates. Then, the cumulative distribution of A_K is obtained by

$$\Pr\{A_K \leq t\} = \Pr\{I_{\Lambda^{1,2}}\big|_{I_{\Lambda^{2,1}} = J(K - J^{-1}(v_K(t)))} \geq v_K(t)\} \tag{11}$$

since $I_{\Lambda^{1,2}}$ is increasing with respect to $I_{\Lambda^{2,1}}$. In the same manner, for given K, we define a random variable B_K denoting the point on the segment of $J^{-1}\left(I_{\Lambda^{1,2}}\right) + J^{-1}\left(I_{\Lambda^{2,1}}\right) = K$ intersecting the h-band, where the observation values of B_K are read in the t_K coordinates. Then, the cumulative distribution of B_K is obtained by

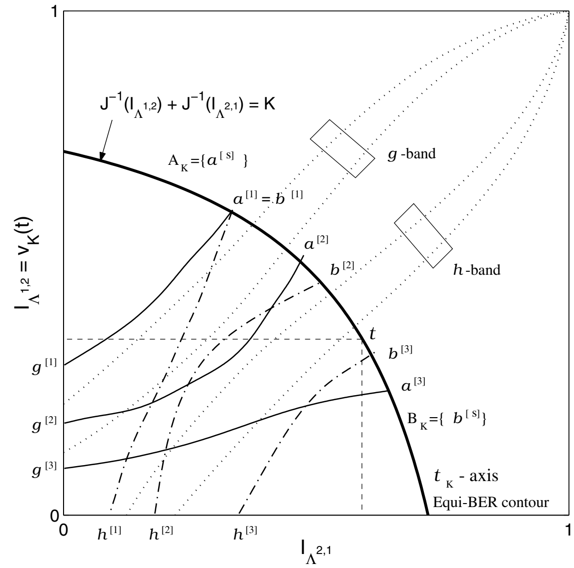

Fig. 5. Relations of equi-BER contour, t_K coordinates, $v_K(\cdot)$, EXIT band chart, A_K and B_K. Sample pairs of $g^{[s]}$ and $h^{[s]}$ with $J^{-1}\left(I_{\Lambda^{1,2[s]}}\right) + J^{-1}\left(I_{\Lambda^{2,1[s]}}\right) \leq K$ are also plotted.

$$\Pr\{B_K \leq t\} = \Pr\{I_{\Lambda^{2,1}}\big|_{I_{\Lambda^{1,2}} = v_K(t)} \leq J\left(K - J^{-1}\left(v_K(t)\right)\right)\}. \tag{12}$$

For given K, let us define α_K as

$$\alpha_K \triangleq \Pr\{A_K \geq B_K\}, \tag{13}$$

which can be computed by using the cumulative distribution of A_K and B_K. Let $I^\infty_{\Lambda^{1,2}}$ and $I^\infty_{\Lambda^{2,1}}$ be $I_{\Lambda^{1,2}}$ and $I_{\Lambda^{2,1}}$, respectively, at convergence of the iterative decoding algorithm. Since the first intersection of $g^{[s]}$ and $h^{[s]}$ is interpreted as the convergence of the iterative decoding algorithm for given $[s]$, it is clear that $I^\infty_{\Lambda^{1,2[s]}}$ and $I^\infty_{\Lambda^{2,1[s]}}$ are read at the first intersection of $g^{[s]}$ and $h^{[s]}$, where $I^\infty_{\Lambda^{1,2[s]}}$ and $I^\infty_{\Lambda^{2,1[s]}}$ are regarded as the sth observation of the random variable $I^\infty_{\Lambda^{1,2}}$ and $I^\infty_{\Lambda^{2,1}}$, respectively. Let us consider sample pairs of of $g^{[s]}$ and $h^{[s]}$ with $J^{-1}(I^\infty_{\Lambda^{1,2[s]}}) + J^{-1}(I^\infty_{\Lambda^{2,1[s]}}) \leq K$ for given K shown in Fig. 5, where $a^{[s]}$ and $b^{[s]}$ denote the sth observation of A_K and B_K, respectively. It is clear that $J^{-1}(I^\infty_{\Lambda^{1,2[s]}}) + J^{-1}(I^\infty_{\Lambda^{2,1[s]}}) \leq K$ if $a^{[s]} \geq b^{[s]}$, but the converse does not hold. Thus,

$$\begin{aligned}\alpha_K &\leq \Pr\left\{\left(J^{-1}\left(I^\infty_{\Lambda^{1,2}}\right) + J^{-1}\left(I^\infty_{\Lambda^{2,1}}\right)\right) \leq K\right\} \\ &= \Pr\left\{Q\left(\sqrt{2R_c\frac{E_b}{N_0} + \left(J^{-1}\left(I^\infty_{\Lambda^{1,2}}\right) + J^{-1}\left(I^\infty_{\Lambda^{2,1}}\right)\right)}\right)\right. \\ &\qquad \left. \geq Q\left(\sqrt{2R_c\frac{E_b}{N_0} + K}\right)\right\}\end{aligned} \tag{14}$$

since $Q(\cdot)$ is decreasing. Let P_e^∞ be the BER performance at the convergence of decoding algorithm. For given K, let us define a "high BER asymptote" ${P_e^h}_K$ as ${P_e^h}_K \triangleq Q\left(\sqrt{2R_c\frac{E_b}{N_0}+K}\right)$. Then, from (10) and (14), we obtain

$$\alpha_K \leq \Pr\left\{P_e^\infty \geq {P_e^h}_K\right\}. \tag{15}$$

Let $\overline{P_e}$ be the average P_e^∞ over all channel realization and interleavers. Then, for each K, we obtain by Bayes' rule

$$\begin{aligned}\overline{P_e} &= E\{P_e^\infty \big| P_e^\infty \geq {P_e^h}_K\} \cdot \Pr\{P_e^\infty \geq {P_e^h}_K\} \\ &\quad + E\{P_e^\infty \big| P_e^\infty < {P_e^h}_K\} \cdot \Pr\{P_e^\infty < {P_e^h}_K\},\end{aligned} \tag{16}$$

where $\overline{P_e}$ is the internal division point of the interval $\left[E\{P_e^\infty \big| P_e^\infty < {P_e^h}_K\}, E\{P_e^\infty \big| P_e^\infty \geq {P_e^h}_K\}\right]$ with the ratio $\Pr\{P_e^\infty \geq {P_e^h}_K\} : \Pr\{P_e^\infty < {P_e^h}_K\}$. Let us choose the "low BER asymptote" P_e^l such that

$$P_e^l \leq E\left\{P_e^\infty \big| P_e^\infty < {P_e^h}_K\right\} \tag{17}$$

for any choice of K. Since ${P_e^h}_K \leq E\{{P_e}^\infty \big| {P_e}^\infty \geq {P_e^h}_K\}$, the lower and upper endpoints of the interval $\left[P_e^l, {P_e^h}_K\right]$ are smaller than those of the interval $\left[E\{{P_e}^\infty \big| {P_e}^\infty < {P_e^h}_K\}, E\{{P_e}^\infty \big| {P_e}^\infty \geq {P_e^h}_K\}\right]$, respectively, for any K. It is clear that ${P_e^h}_K \cdot \alpha_K + P_e^l \cdot (1-\alpha_K)$ is the interval division point of the interval $\left[P_e^l, {P_e^h}_K\right]$ with the ratio $\alpha_K : 1-\alpha_K$. Then, by comparing the endpoints of above two intervals and their division ratios related by (15), it is clear that $\overline{P_e} \geq {P_e^h}_K \cdot \alpha_K + P_e^l \cdot (1-\alpha_K)$ for any K. Thus, we have

$$\overline{P_e} \geq \sup_K \left\{{P_e^h}_K \cdot \alpha_K + P_e^l \cdot (1-\alpha_K)\right\}. \tag{18}$$

There may exist many ways of choosing P_e^l. In this paper, we choose the free distance asymptote proposed by Perez *et al* [9] as P_e^l, which is

$$P_e^l \triangleq \frac{N_{\text{free}}\tilde{w}_{\text{free}}}{N} Q\left(\sqrt{2R_c d_{\text{free}}\frac{E_b}{N_0}}\right), \tag{19}$$

where d_{free} is the free distance, N_{free} is the average multiplicity of free distance codewords over all possible random interleavers, and $\tilde{w}_{\text{free}}$ is the average weight of the information sequences causing free distance codewords. For each K, we compute α_K by using the cumulative distributions of A_K and B_K by way of (11) and (12) which are measured from the EXIT band chart. The lower bounds on the average BER obtained in (18) are plotted together with the BER obtained by the full simulation of the iterative turbo decoding algorithm in Fig. 6. As we can see in Fig. 6, the proposed lower bounds are in reasonable agreement with the simulated BER performance curves even in the waterfall region. The critical factor to improve the lower bound is finding a tighter P_e^l to the simulated BER performance curve at high $\frac{E_b}{N_0}$. One of ideas is adding up the free distance asymptote, the second free distance asymptote and so on to obtain P_e^l, i.e., $P_e^l = \sum_{d=d_{\text{free}}}^{d'} \frac{N_d\tilde{w}_d}{N} Q\left(\sqrt{2R_c d\frac{E_b}{N_0}}\right)$, for appropriately chosen $d' > d_{\text{free}}$.

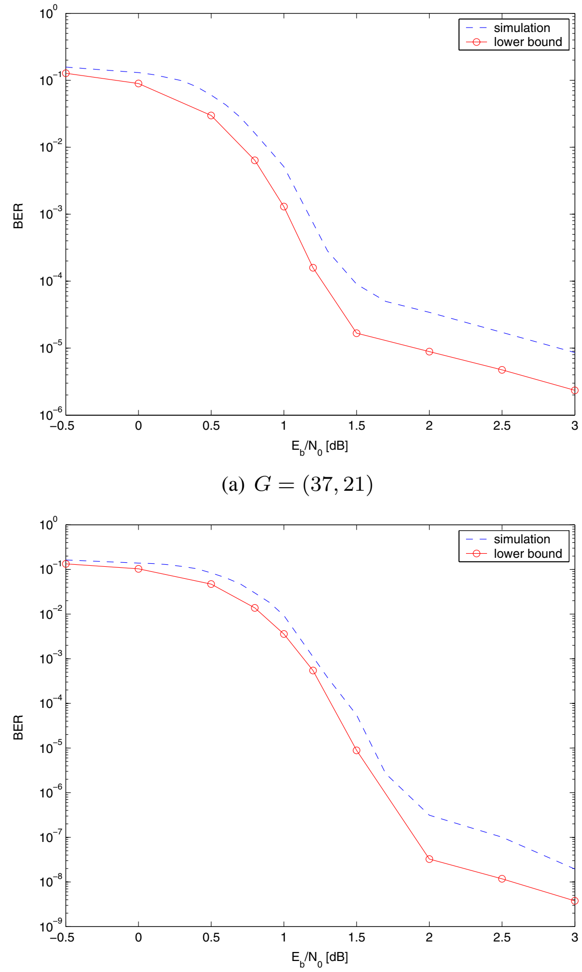

(a) $G = (37, 21)$

(b) $G = (31, 27)$

Fig. 6. The lower bounds on the BER performance of turbo codes for two sample generators with $N = 1024$ and $R_c = 1/2$.

V. Conclusion

We proposed an EXIT band chart which can describe the probabilistic convergence behavior of the iterative decoding algorithm. Then, by using the proposed EXIT band chart, we obtained a lower bound on the average BER performance of the finite-length turbo codes which has a gentle waterfall over a wide waterfall region. The obtained lower bound is in reasonable agreement with the BER obtained by the simulations of the iterative decoding algorithm. The proposed method can generally be applied to obtain the lower bound on the BER performance of iteratively decoded turbo-like codes with short information block which result in the gentle waterfall.

References

[1] C. Berrou, A. Glavieux, and P. Thitimajshima, "Near shannon limit error-correcting coding and decoding: Turbo-codes," in *Proc. 1993 IEEE Int. Conf. on Communication*, (Geneva, Switzerland), pp. 1064–1070, May 1993.

[2] S. ten Brink, "Convergence behavior of iteratively decoded parallel concatenated codes," *IEEE Trans. Commun.*, vol. 49, pp. 1727–1737, Oct. 2001.

[3] T. Richardson, A. Shokrollahi, and R. Urbanke, "Design of provably good low-density parity-check codes." submitted to IEEE Trans. Inform. Theory.
[4] H. E. Gamal and J. A. Hammons, "Analyzing the turbo decoder using the gaussian approximation," *IEEE Trans. Inform. Theory*, vol. 47, pp. 671–686, Feb. 2001.
[5] D. Divsalar, S. Dolinar, and F. Pollara, "Iterative turbo decoder analysis based on density evolution," *IEEE J. Select. Areas in Commun.*, vol. 19, pp. 891–907, May 2001.
[6] 3GPP TS 25.212, Available at http://www.3gpp.org.
[7] J. W. Lee and R. E. Blahut, "Analysis of the extrinsic values in the finite length turbo decoding," in *Proc. 36th Conf. Information Sciences and Systems*, (Princeton, NJ), Mar. 2002.
[8] J. W. Lee and R. E. Blahut, "Bit error rate estimate of finite length turbo codes," in *Proc. IEEE 2003 Int. Conf. on Communication*, (Anchorage, AK), May 2003.
[9] L. Perez, J. Seghers, and D. Costello, "A distance spectrum interpretation of turbo codes," *IEEE Trans. Inform. Theory*, vol. 42, pp. 1698–1709, Nov. 1996.

